## Nano Scale Disruptive Silicon-Plasmonic Platform for Chip-to-Chip Interconnection

# Plasmonic components integration to demonstrate chip-to-chip interconnect

Milestone no.: M42
Due date: 04/31/2015
Actual Submission date: 08/03/2015
Authors: ETHZ
Work package(s): WP6
Distribution level: RE[1] (NAVOLCHI Consortium)
Nature: document, available online in the restricted area of the NAVOLCHI webpage

## List of Partners concerned

| Partner number | Partner name | Partner short name | Country | Date enter project | Date exit project |
|---|---|---|---|---|---|
| 1 | Karlsruher Institut für Technologie | KIT | Germany | M1 | M36 |
| 2 | INTERUNIVERSITAIR MICRO-ELECTRONICA CENTRUM VZW | IMEC | Belgium | M1 | M36 |
| 3 | TECHNISCHE UNIVERSITEIT EINDHOVEN | TU/e | Netherlands | M1 | M36 |
| 4 | RESEARCH AND EDUCATION LABORATORY IN INFORMATION TECHNOLOGIES | AIT | Greece | M1 | M36 |
| 5 | UNIVERSITAT DE VALENCIA | UVEG | Spain | M1 | M36 |
| 6 | STMICROELECTRONICS SRL | ST | Italy | M1 | M36 |
| 7 | UNIVERSITEIT GENT | UGent | Belgium | M1 | M36 |

[1] **PU** = Public
**PP** = Restricted to other programme participants (including the Commission Services)
**RE** = Restricted to a group specified by the consortium (including the Commission Services)
**CO** = Confidential, only for members of the consortium (including the Commission Services)

## *Deliverable Responsible*

Organization: ETH Zurich
Contact Person: Claudia Hoessbacher
Address: Institue of Electromagnetic Fields (IEF)
ETZ K 93
Gloriastrasse 35
Gloriastrasse 35
Switzerland
Phone: +41 44 632 67 68
E-mail: choessbacher@ethz.ch

## *Executive Summary*

Milestone 42 concerns the plasmonic components integration. In this context, deliverable 6.4 was submitted in accordance with the NAVOLCHI “Description of Work”. The plasmonic modulators were integrated with their driving electronics to a single transmitter module. Furthermore, Si-Ge photodiodes were assembled with transimpedance amplifiers, thus realizing a full receiver. A hybrid integration approach with electrical wire bonds were used on both sides. As a first step, both modules were tested independently. The transmitter and receiver were successfully operated at 4 × 10 Gbit/s and 3 x 28 Gbit/s, respectively.

## *Change Records*

| Version | Date | Changes | Author |
|---|---|---|---|
| 1 (submission) | 2015-08-03 | | Claudia Hoessbacher |
| 2 | 2015-09-21 | | Claudia Hoessbacher |

# *Plasmonic components integration to demonstrate chip-to-chip interconnect*

## Transmitter

On the transmitter side, the plasmonic modulators were integrated with their driving electronics in a single package as shown in Fig. 1(a). A customized copper housing was fabricated to assemble the plasmonic and electronic components. Electrical wire bonding interconnected the electronic board with the plasmonic modulator array, see Fig. 1(b). To minimize the length of the wirebonds, the plasmonic chip was diced to a size of 5 x 20 mm and placed in a cavity in the middle of the housing. The data signal was fed to the electronic board via high-speed K-connecters at the edge of the housing. On the board the signal was amplified by four RF amplifiers, before being sent to the plasmonic modulator array. As an external heat sink, a copper block was placed below the transmitter. It further adjusted the height to our characterization setup. To allow for easy testing, PCB and housing were not minimized in size. A multicore fiber (MCF) and a standard single mode fiber (SMF) were used as an optical input and output, respectively.

The applicability plasmonic transmitter in communication systems was verified by data modulation experiments. Data signals with binary phase shift keying (BPSK) at 10 Gbit/s were generated. Four CW laser sources (1549.3 nm to 1551.9 nm, $\Delta\lambda \approx 1$ nm) were coupled to the array via the MCF. Two digital-to-analog converters (72 GSa/s, 6 bit) generated uncorrelated, differential signals D1 and D2 (pulse shape: square-root-raised cosine, roll off $\alpha = 1$) with De Bruijn bit sequences (DBBS 11). $D_1, D_2, \overline{D}_1$, and $\overline{D}_2$ were fed to the single ended transmitter. The four channels were received sequentially with a standard single mode fiber in a coherent receiver. Pre-distortion and post-equalization of the electrical signal was used to mitigate the frequency dependence of the RF amplifiers and the DACs. Fig. 3 depicts the measured optical eye diagrams and constellation diagrams for all four channels at 10 Gbit/s. All channels have bit error ratios (BERs) below the FEC limit of $2\times10{-}3$ (7 % overhead); no error was detected within the 10 million recorded bits for channel 1 and 3.

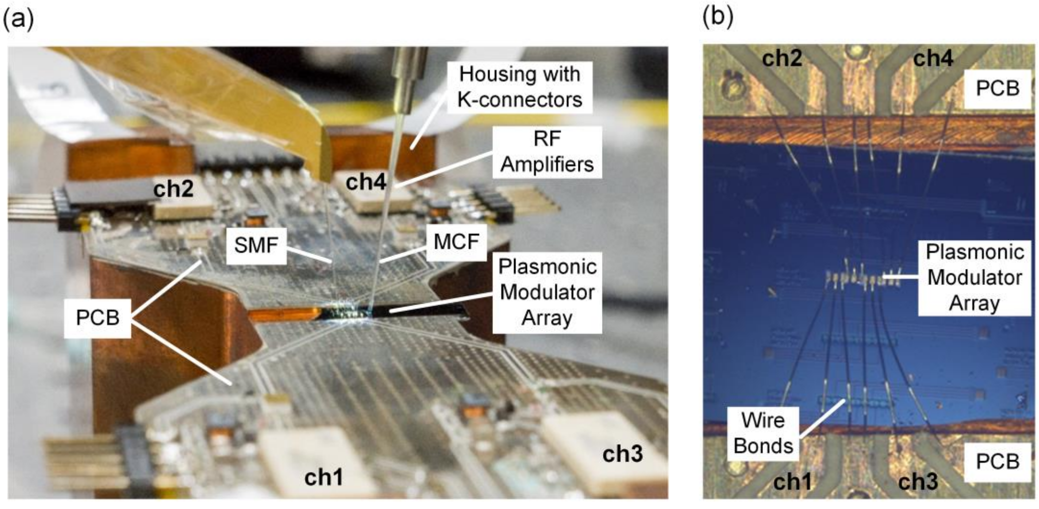


**Fig. 1** Transmitter. **(a)** Customized package with plasmonic modulator array and PCB containing driving electronics. **(b)** Plasmonic modulators wirebonded to the PCB.

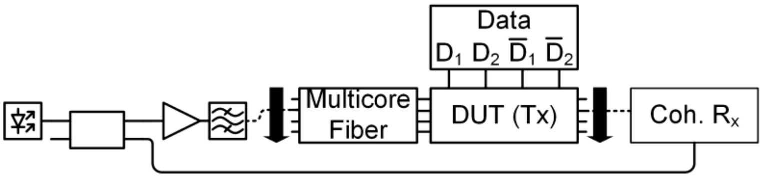


**Fig. 2** Experimental setup for data modulation experiments. Laser light at different wavelengths ($\Delta\lambda \approx 1$ nm at $\lambda \approx 1550$ nm) was amplified and coupled via a multicore fiber to the transmitter (Tx). Four electrical data streams were fed to the Tx by two independent DACs. The modulated light of the channel under test was received by a coherent receiver. The laser source was also used as local oscillator in the receiver.

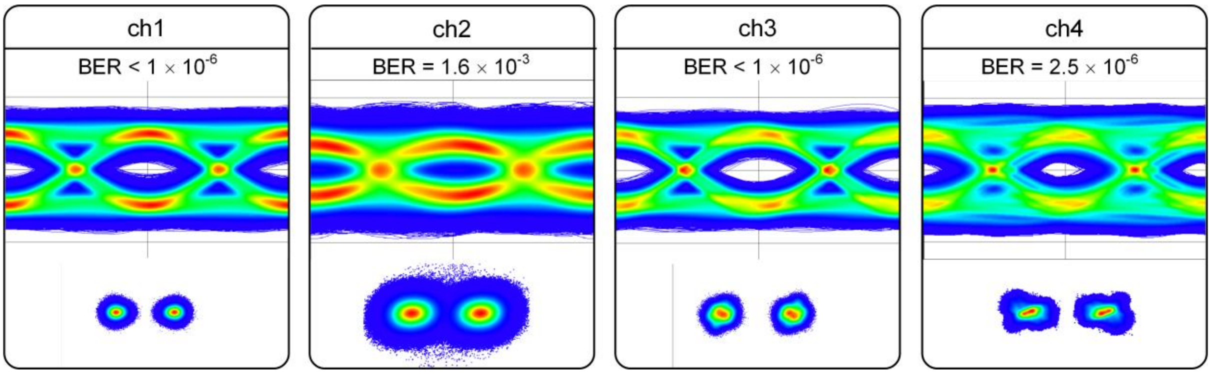


**Fig. 3** Optical eye and constellation diagrams with bit error ratios (BER) of the data experiments (BPSK) at data rates of 10 Gbit/s. All four channels have a BER below the FEC limit of $2\times10{-}3$.

## *Receiver*

On the receiver side, IMEC's Si-Ge photodiodes (PD) were used and wire bonded to a 4 channel 28 Gb/s transimpedance limiting amplifier (TIA) array, see Fig. 4. The photonic and electronic components were assembled on an evaluation board. To minimize the length of the wirebonds, the photonic chip was diced close to the contact pads and placed in proximity to the electronic chip. Channel 2 could not be bonded, though, since the arrangement of the anode and cathode contact pads on the optical and the electronic chip did not perfectly match. The optical signal was coupled in via a standard single mode fiber.

The receiver was tested in data experiments as shown in Fig. 5. Data signals with Non-Return-to-Zero (NRZ, rectangular) at 28 Gbit/s were generated by an arbitrary waveform generator and a commercial modulator at 1550 nm wavelength. The three channels were tested sequentially with a standard single mode fiber. The signal was recorded with a digital communication analyzer. TIA settings were optimized for high quality factors and low jitter. Fig. 6 depicts the measured optical eye diagrams and quality factors for the three channels. The eye diagrams are convincingly open.

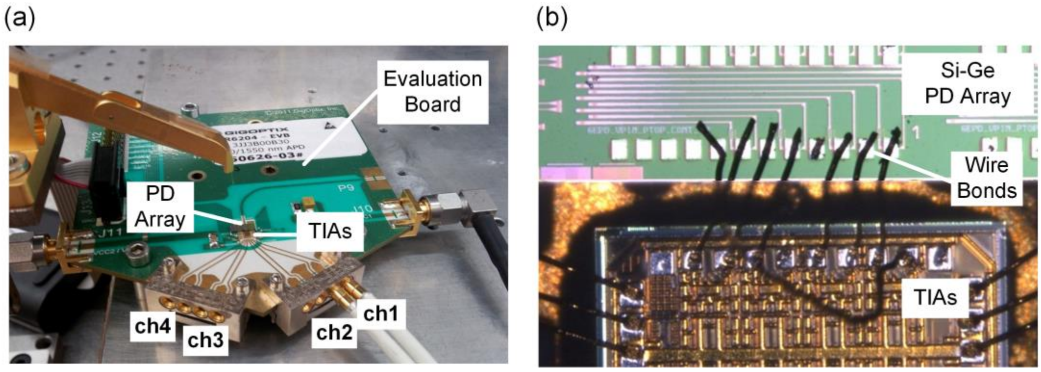


**Fig. 4** Receiver **(a)** Evaluation board with Si-Ge photodiode array and PCB containing electronics. **(b)** Photodiodes wirebonded to the PCB. Channel 2 could not be bonded, since the arrangement of the anode and cathode contact pads on the optical and the electronic chip did not perfectly match.

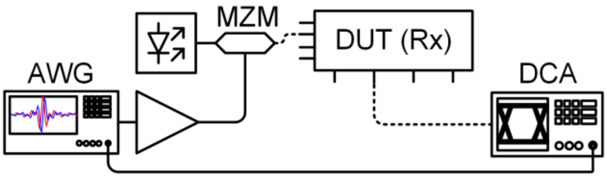


**Fig. 5** Experimental setup for data modulation experiments. Laser light at 1550 nm was coupled to a commercial Mach-Zehnder modulator (MZM). Electrical data streams were generated by an arbitrary waveform generator (AWG) and amplified, before being sent to the MZM. The modulated light was sent to the channel under test of the receiver (Rx). The received signal was measured with a digital communication analyser (DCA).

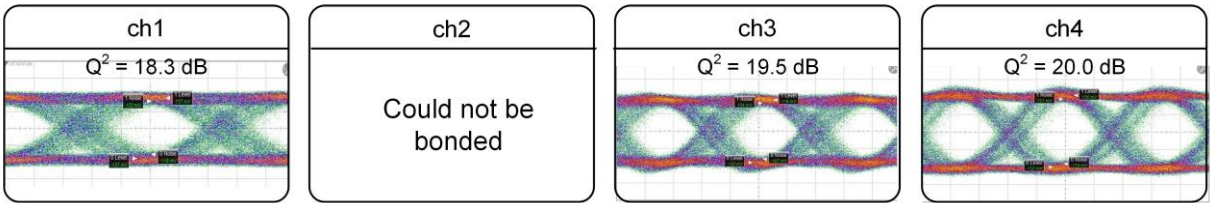


**Fig. 6** Optical eye diagrams with quality factor ($Q^2$) of the data experiments (NRZ, rectangular) at data rates of 28 Gbit/s. Channel 2 could not be bonded (see **Fig. 4**), so no data experiment was carried out. Channel 2,3,4 show open eye diagrams.